

Chapter V
RESULTS AND ANALYSIS



5.1 Introduction

The result from the experiment are the gain measurement of each block diagram as described in Chapter II, the motor time constant, the performance of the system, and the calculation of some factors in the overall transfer function. The analysis of the system can be determined from the transfer function.

5.2 Gain Measurement

Detector Gain

Consider the moving part of the system as shown in Figure 5.1. The detector angle θ is set at a maximum value of 45° as described in Chapter IV.

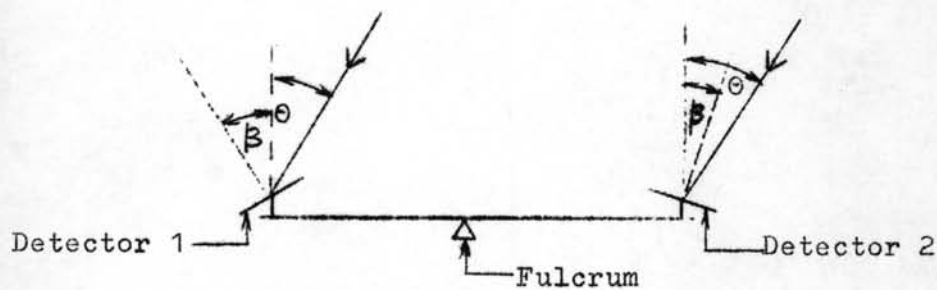


Figure 5.1. Moving Part of the System.

Table 5.1 displays the measurement of the difference voltage ($V = V_1 - V_2$) at various values of angle θ .

Table 5.1 Difference voltages at various light angles.

Angle (θ)	Difference voltages "v" (mv.)	*Short circuit currents(ma.)	**Radiation (W/m ²)
10	0.05	5.5	261.25
20	0.12	5.0	237.5
30	0.20	4.5	213.75
40	0.25	4.1	194.75
50	0.30	3.5	166.25
60	0.35	3.0	142.5
70	0.36	2.5	118.75
80	0.40	2.2	104.5
90	0.40	1.8	85.5
-10	-0.04	5.5	261.25
-20	-0.1	5.0	237.5
-30	-0.22	4.5	213.75
-40	-0.26	4.0	190
-50	-0.32	3.5	166.25
-60	-0.36	3.2	152
-70	-0.38	2.6	123.5
-80	-0.40	2.3	109.25
-90	-0.40	1.9	90.25

*A short circuit current is measured on a solar cell(S7M2) which lied in the same direction as the flat plate.

**Radiation (in W/m²) is calculated by multiplying a short circuit current with slope of a solar cell (S7M2)'s characteristic. The slope is 0.0475 W/m²/A.

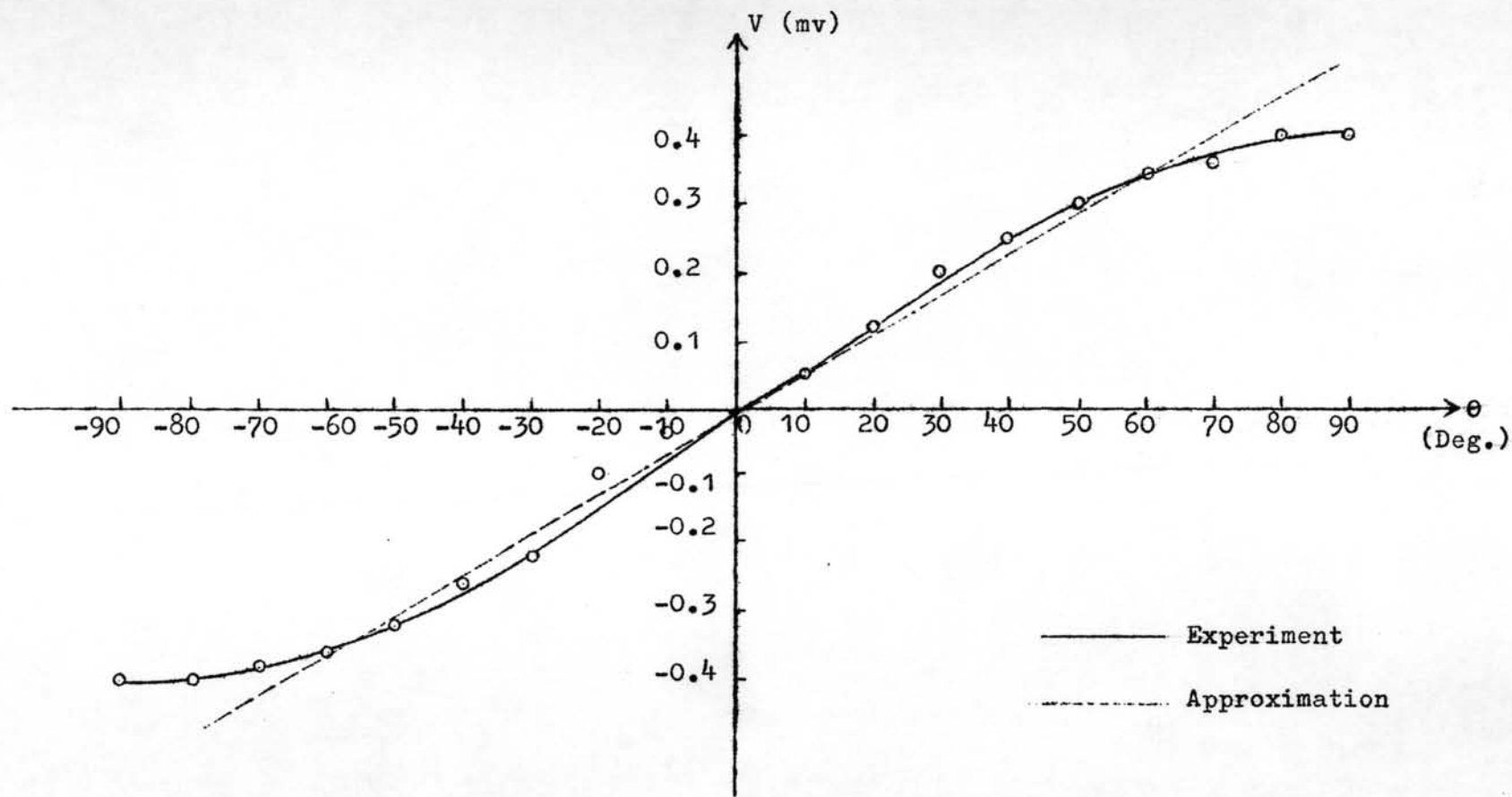


Figure 5.2. A Plot of Difference Voltage ($V = V_1 - V_2$) VS. light angle.

Figure 5.2 illustrates the relationship between the difference voltage and the light angle. From the graph, the detector gain (K_1) can be determined .

The slope can be approximated by a straight line drawn between angle range $\pm 60^\circ$. Then, the detector gain is :

$$\begin{aligned} K_1 &= \frac{V}{\theta_c} , \\ &= \frac{0.35 \times 10^{-3}}{\pi/3} , \\ &= 0.334 \times 10^{-3} . \end{aligned} \quad \text{Volt/radian}$$

This value is obtained when the solar radiation is about 285 W/m^2 , the figure which approximates the yearly average of solar radiation in Thailand. The yearly average of solar radiation in Thailand is approximately 250 W/m^2 .³

Gain of Operational Amplifier and Power Amplifier

The gain of the operational amplifier and power amplifier (K_2) had already calculated in Chapter IV. That is :

$$\begin{aligned} K_2 &= V_m/V , \\ &= 8,000 . \end{aligned}$$

Motor Gain

The motor used in the system is a 1 rpm., 12 V, d.c. permanent-magnet motor. The gain (K_m) can be determined from its specification.

$$K_m = \frac{1}{K_c} ,$$

where $K_c =$ voltage constant of the motor in Volt/(rad./sec),

$$K_{mi} = \frac{1}{12/2 /60} ,$$

$$= \frac{2}{12 \times 60} ,$$

$$= 8.727 \times 10^{-3} \text{ rad./volt-sec}$$

Gear Ratio

$$\text{The gear ratio (M)} = \frac{N_1}{N_2} = 2.$$

Motor Time Constant

The time constant of the motor with gear reduction and load is the time required for an exponential component of a transient response of motor. The experimental set-up used to determine the time constant is shown in Figure 5.3.

The response obtained from CRO can be approximately drawn in Figure 5.4. The measured time constant is the mechanical time constant (T_m) which involves the inertia of the motor and the friction components. It is measured on the graph as the time for the current to drop from the maximum to the steady-state value. For this motor, it is 25 ms.

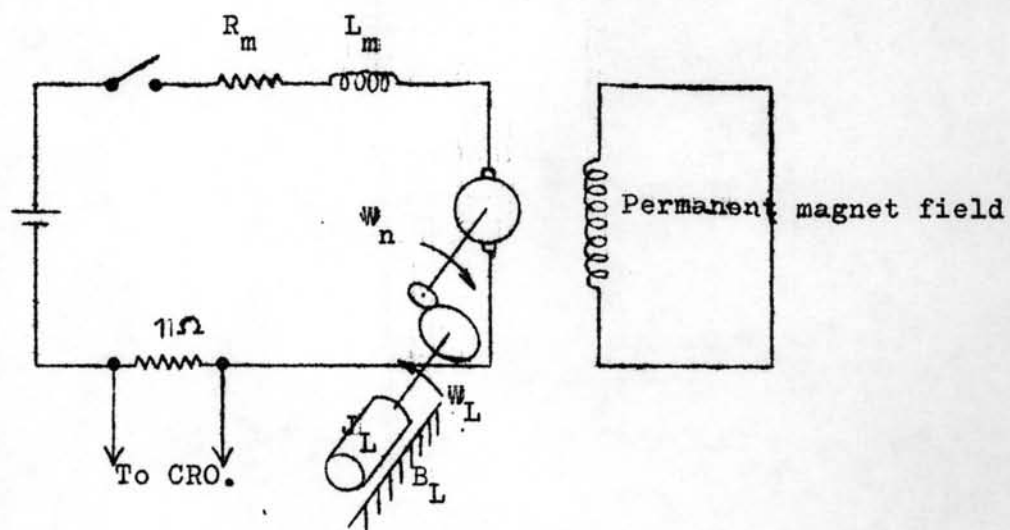


Figure 5.3 Experiment on Motor Time Constant Measurement.

Analysis of the Complete System

The block diagram of the complete system as shown in Figure 2.2 can be replaced by a single block diagram as shown in Figure 5.5 .

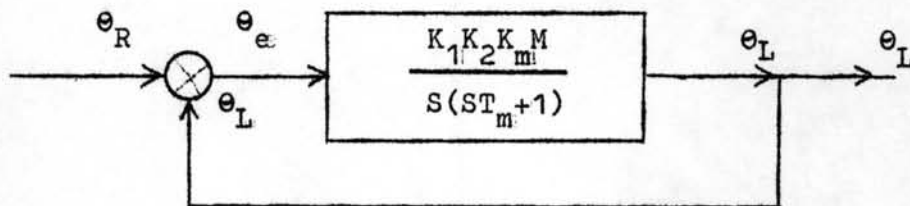


Figure 5.5 Block Diagram of the Complete System.

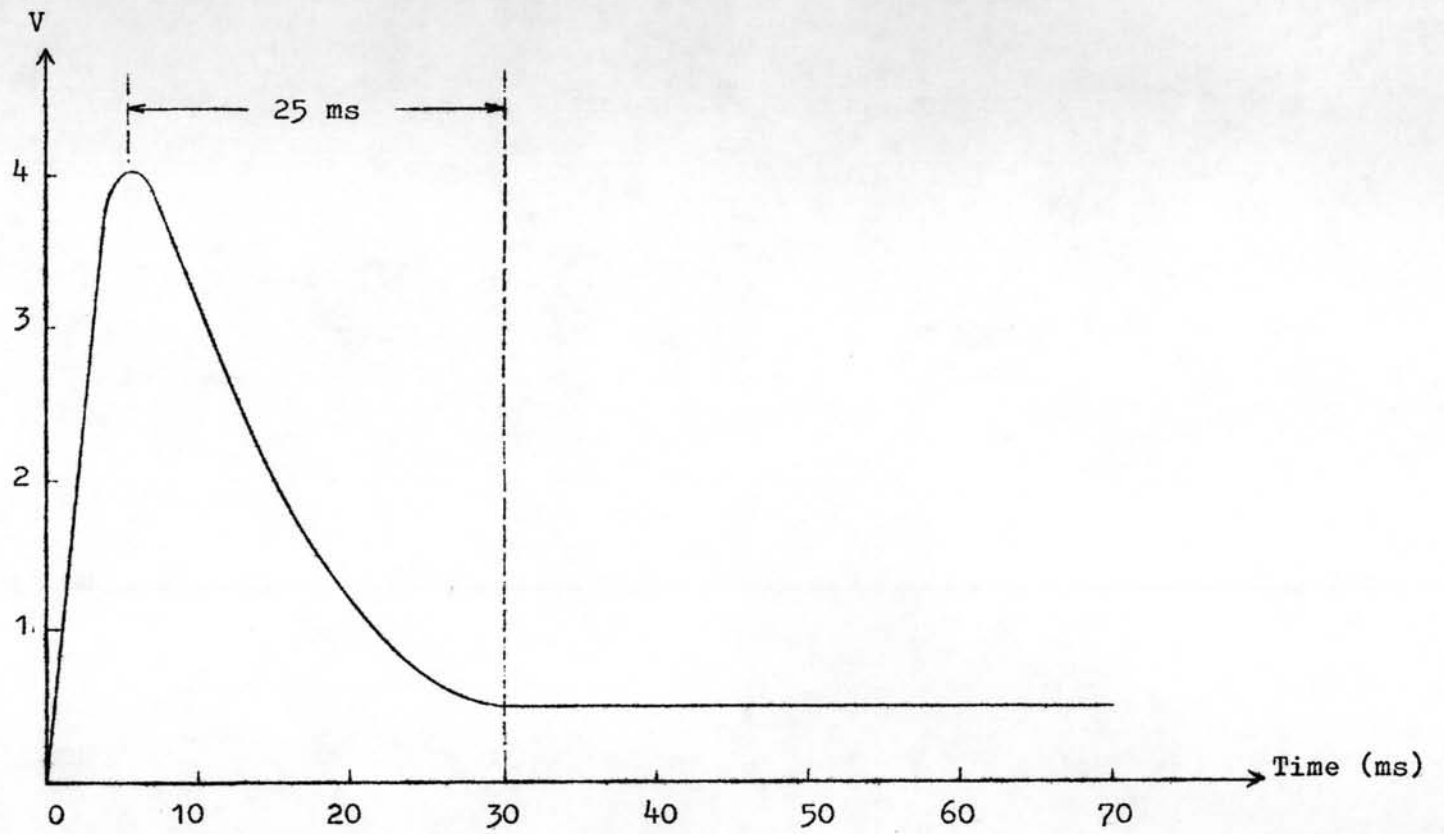


Figure 5.4 Motor Time Constant with Load.

$$\begin{aligned}
 \text{Transfer function} &= \frac{\theta_L}{\theta_R} , \\
 &= \frac{K_1 K_2 K_m / T_m}{s^2 + s/T_m + K_1 K_2 K_m / T_m} , \\
 &= \frac{\omega_n^2}{s^2 + 2\zeta\omega_n s + \omega_n^2} .
 \end{aligned}$$

where ω_n = undamped natural frequency ,

$$= \sqrt{K_1 K_2 K_m / T_m} ,$$

$$= \sqrt{\frac{0.334 \times 10^{-3} \times 8,000 \times 8,727 \times 10^{-3}}{25 \times 10^{-3}}} ,$$

$$= \sqrt{1.865} ,$$

$$= 1.36 \quad \text{cycle/sec} ,$$

ζ = damping ratio ,

$$= \frac{1}{2\omega_n} \cdot \frac{1}{T_m} ,$$

$$= 14.7 .$$

The damping ratio exceeds 1; the system is overdamped and consequently , the system is stable. The transfer function of the system may be evaluated as follows :-

$$\begin{aligned}
 \frac{\theta_L}{\theta_R} &= \frac{1.865}{s^2 + 2 \times 14.7 \times 1.36 s + 1.865} , \\
 &= \frac{1.865}{s^2 + 39.985 s + 1.865} .
 \end{aligned}$$

In addition to stability, sensitivity and accuracy, control engineers are always quite concerned with the transient response of a feedback system. The response of the second-order system

to a unit step and unit ramp input can be obtained by substituting $\theta_R(S)$ with $\frac{1}{S}$ and $\frac{1}{S^2}$ respectively.

$$1. \text{ Unit Step Input } \theta_R(S) = \frac{1}{S}$$

$$\begin{aligned} \theta_L(S) &= \frac{1}{S} \cdot \frac{1.865}{s^2 + 39.985s + 1.865} \\ &= \frac{1}{S} \cdot \frac{1.865}{(s+0.0467)(s+39.9333)} \\ &= \frac{A}{S} + \frac{B}{s+0.0467} + \frac{C}{s+39.9333} \end{aligned}$$

Using Residue's Theorem; the constants A, B, and C are as follows :

$$\begin{aligned} A &= 1 \\ B &= -1.0012 \\ C &= 0.0012 \end{aligned}$$

and then

$$\theta_L(S) = \frac{1}{S} - \frac{1.0012}{s+0.0467} + \frac{0.0012}{s+39.9333}$$

The time domain response of the output is :-

$$\theta_1(t) = 1 - 1.0012 e^{-0.0467t} + 0.0012 e^{-39.9333t}$$

$$2. \text{ Unit Ramp Input } \theta_R(S) = \frac{1}{S^2}$$

$$\begin{aligned} \theta_L(S) &= \frac{1}{S^2} \cdot \frac{1.865}{(s+0.0467)(s+39.9333)} \\ &= \frac{A}{S} + \frac{B}{S^2} + \frac{C}{s+0.0467} + \frac{D}{s+39.9333} \end{aligned}$$

Using Residue's Theorem, the constants A, B, C and D are as follows :

$$A = -21.44,$$

$$B = 1,$$

$$C = 21.44,$$

$$D = -0.31 \times 10^{-4}.$$

and then,

$$\theta_L(s) = \frac{-21.44}{s} + \frac{1}{s^2} + \frac{21.44}{s + 0.0467} - \frac{0.31 \times 10^{-4}}{s + 39.9333}$$

The time domain response of the output is :

$$\begin{aligned} \theta_L(t) &= -21.44 + t + 21.44e^{-0.0467t} - 0.31 \times 10^{-4}e^{-39.9333t}, \\ &= t - 21.44(1 - e^{-0.0467t}). \quad (\text{approx.}) \end{aligned}$$

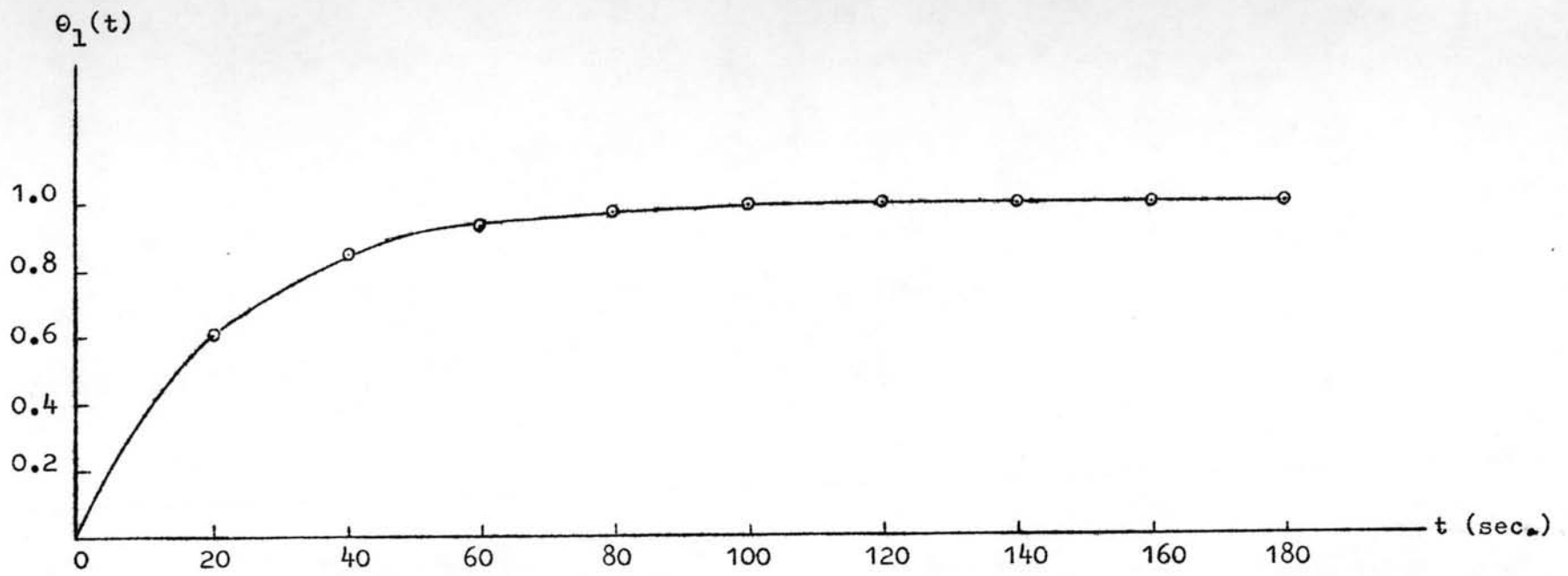


Figure 5.6 (a) Response to a Unit Step Input.

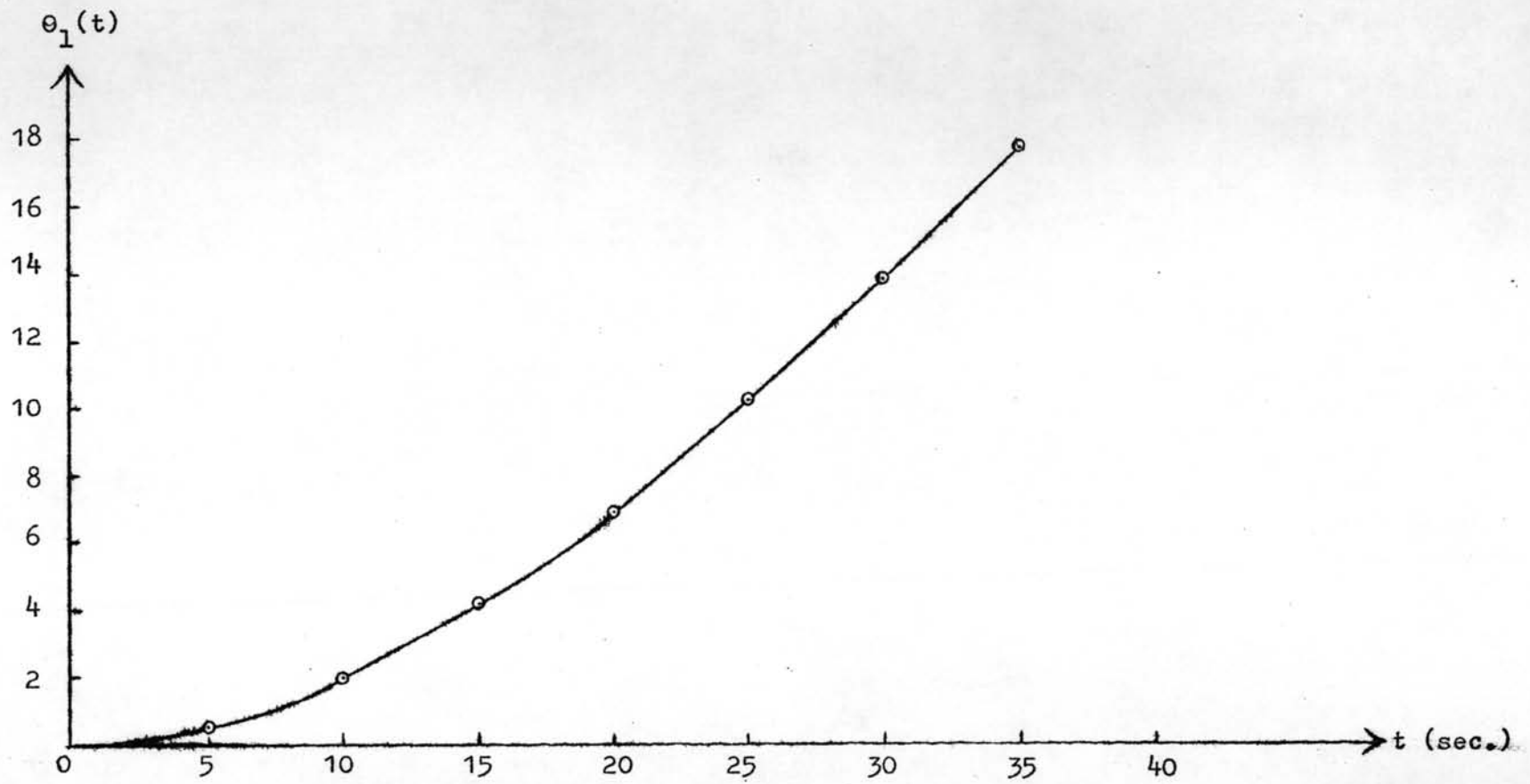


Figure 5.6 (b) Response to a Unit Ramp Input.

Measurement of the Performance

To determine the performance of the tracking system, it is necessary to measure simultaneously the tracked angle of the system and the position of the sun. The results are tabulated in Table 5.2.

From Table 5.2, the average tracked error angle is approximately ± 1 degree. The tracked error angle is very small because the measurement was performed on a calm day. In the windy day, because of the wind, further error may be observed due to the increasing effect of gear backlash.

Table 5.2 Measurement of the Performance

Time	Tracked Angle of the- System (degree)	Position of the- Sun (degree)	Absolute Errors
10.00	115	114	1
10.15	112	111	1
10.30	110	108	2
10.45	107	106	1
11.00	102	102	0
11.15	99	98	1
11.30	95	95	0
11.45	92	92	0
12.00	90	90	0
12.15	86	86	0
12.30	82	82	0
12.45	77	79	2
13.00	75	75	0
13.15	73	71	2
13.30	70	66	4
13.45	64	63	1
14.00	58	60	2
14.15	55	56	1
14.30	52	52	0
14.45	48	49	1
15.00	43	45	2
15.15	40	42	2

Note : The measured angle, indicated by the pointer attached to the scale, changes from 180° when the sun is in the East to 0° when the sun moves to the West. The measurement was carried out on May 2, 1977 on the roof of the E.E. building.

Analysis of Response due to the Effect of Nonlinearities

The preceding section describes the analysis of the response when the system is assumed to be linear. This section illustrates the describing function concepts developed for nonlinear control system. Nonlinearities arise in this system because some of the comprising components are imperfect. For example, the servo amplifier becomes saturated when the input signal gets sufficiently large. It is rather difficult to formulate an explicit expression relating the output to an input. The nonlinearity is simulated by a function generator.

Another type of nonlinearity occurring commonly in a moving mechanical system is the friction opposing motion. Such nonlinearities are the gear backlash and the coulomb friction. The motor used has a nonlinear characteristic because of the dead zone effect. The block diagram of the system containing nonlinear elements is shown in Figure 5.7 and 5.8.

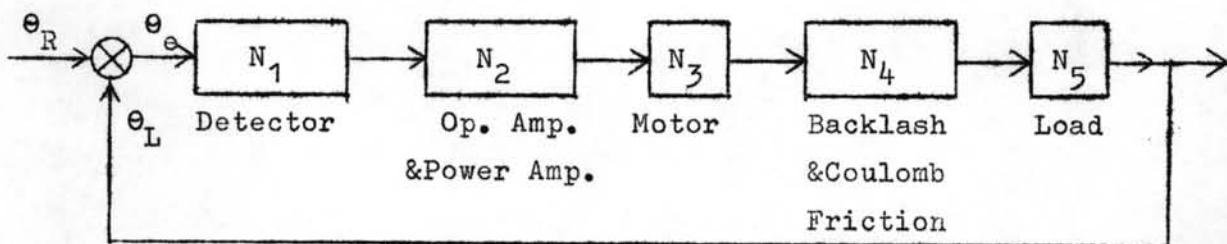


Figure 5.7. The Block Diagram of a System Containing Nonlinear Elements.

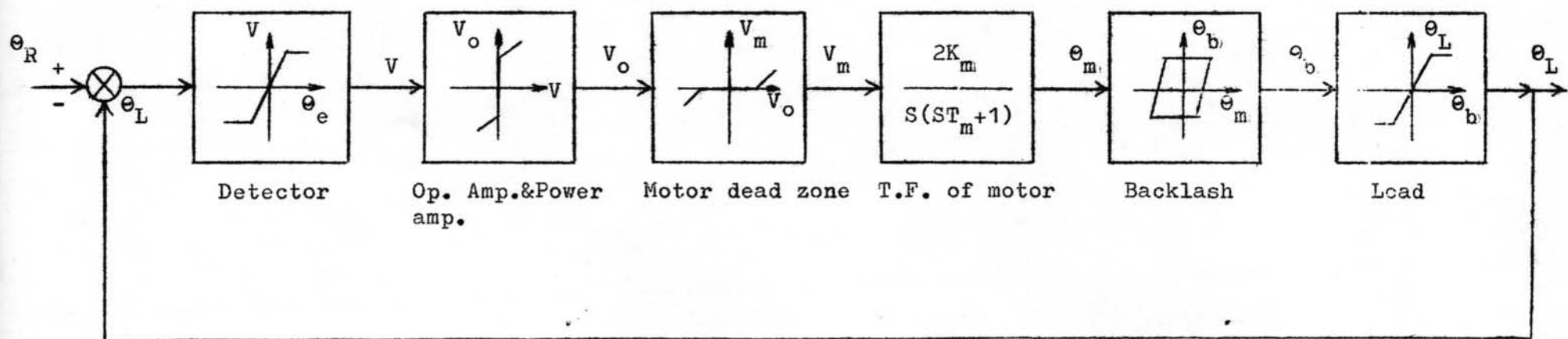


Figure 5.8 Block Diagram with Nonlinear Characteristics.

The analog representation for several nonlinearities is shown in appendix B. For the transfer function of motor; it can be represented as follows :-

$$\text{T.F. of motor} = \frac{\theta_m}{V_m} = \frac{2K_m}{S(ST_m + 1)}$$

$$\begin{aligned} \ddot{\theta}_m &= \frac{2K_m V_m}{T_m} - \frac{\dot{\theta}_m}{T_m} \\ &= 0.7 V_m - 40 \dot{\theta}_m \end{aligned}$$

$$\text{where } K_m = 8.727 \times 10^{-3}$$

$$T_m = 25 \text{ ms.}$$

The analog representation for the transfer function of motor is shown in Figure 5.9 .

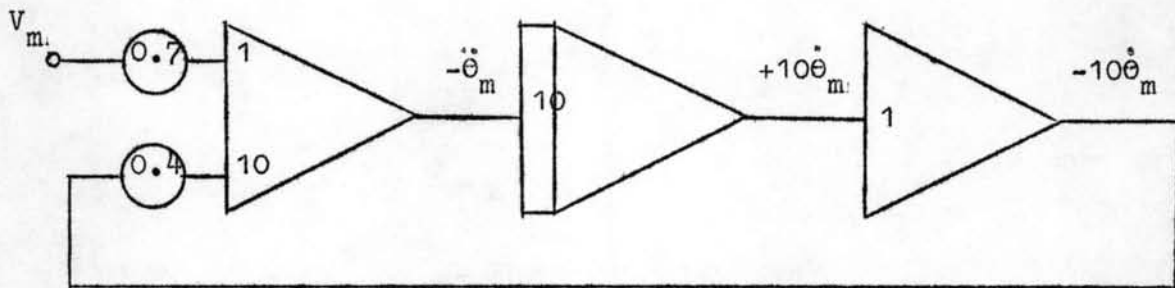


Figure 5.9. An Analog Representation for the T.F. of the Motor.

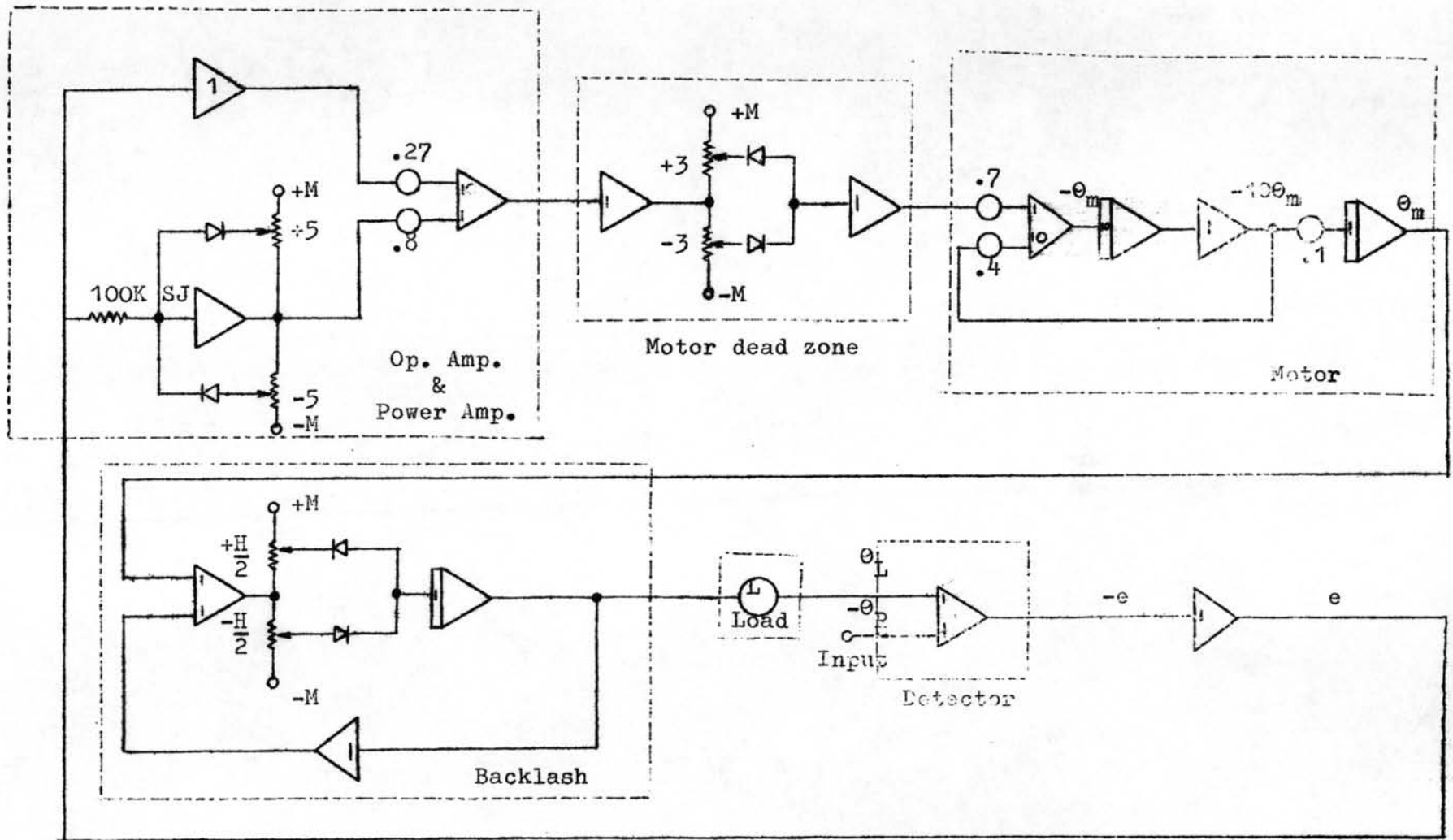


Figure 5.10 Analog Computer Diagram for Simulation of the System.

To determine transient response of the system, a simulation technique can be used. The analog simulation of nonlinear systems is accomplished in essentially the same manner as in the analog simulation of linear systems, except that some of the block in the diagram may now incorporate nonlinearities. The overall program for analog computer simulation of the system is shown in Figure 5.10, where the threshold nonlinearity (dead zone) is represented by its characteristics only and the effect of disturbances such as the gear backlash and the coulomb friction inserted between the motor output and the load are taken into consideration.

The test results obtained by the analog computer simulation are shown in Figure 5.11 and Figure 5.12. Recording of input, error and output for small and larger backlash are also shown. Observation reveals that the steady state error of this system with nonlinear characteristics and backlash goes to zero for both input. The system response exhibits no overshoots and takes a long time to reach its final value. This overdamping feature illustrates the stability of the system.

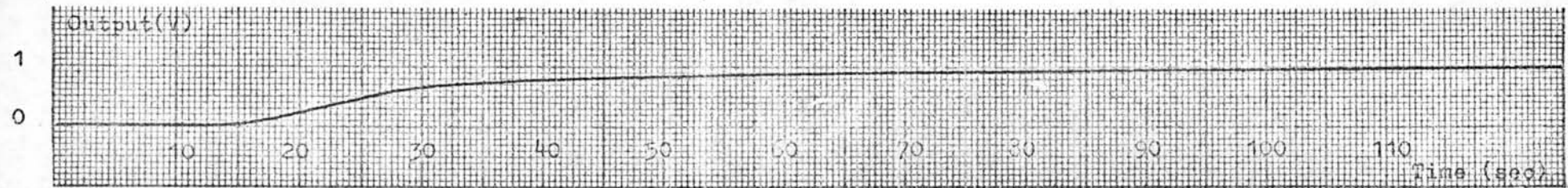
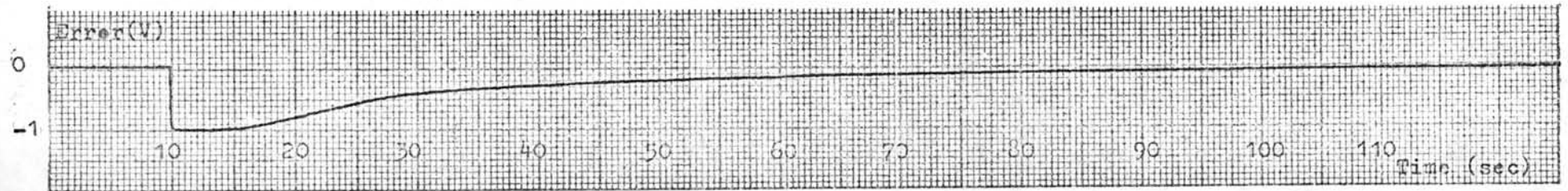
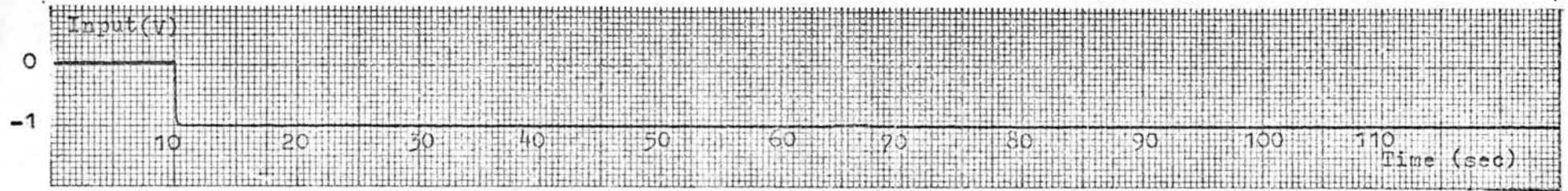
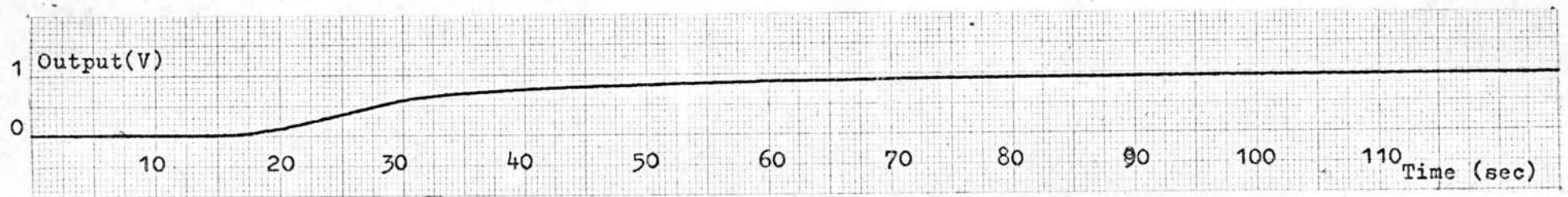
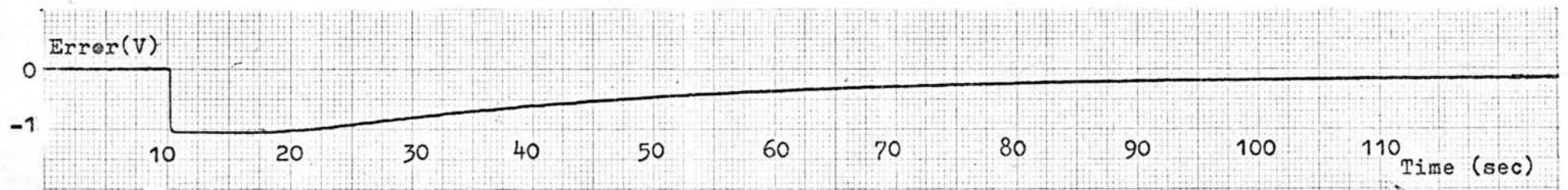
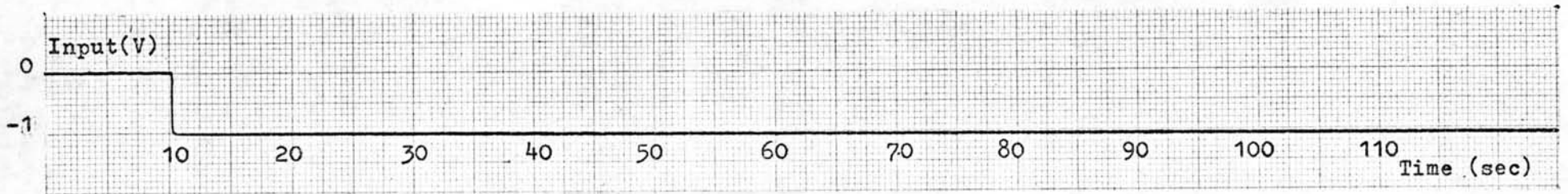
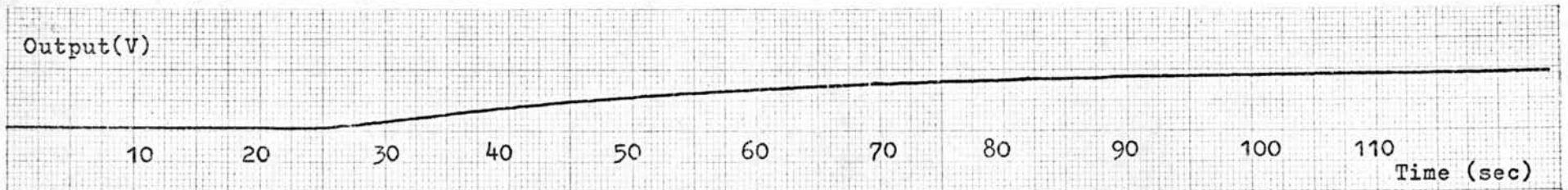
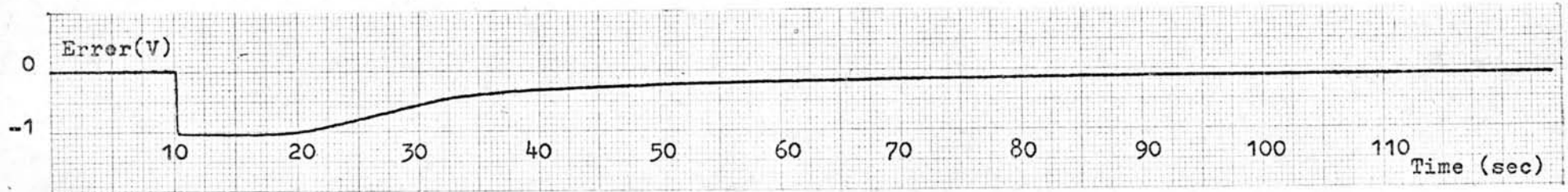
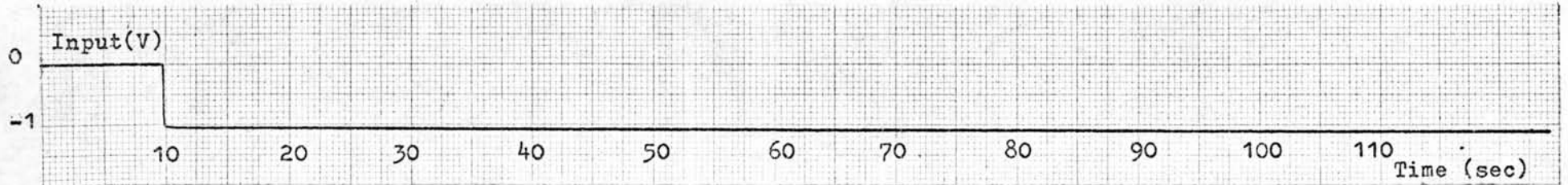


Figure 5.11. (a). Step response without backlash



(b). Step response with small backlash



(c). Step response with larger backlash

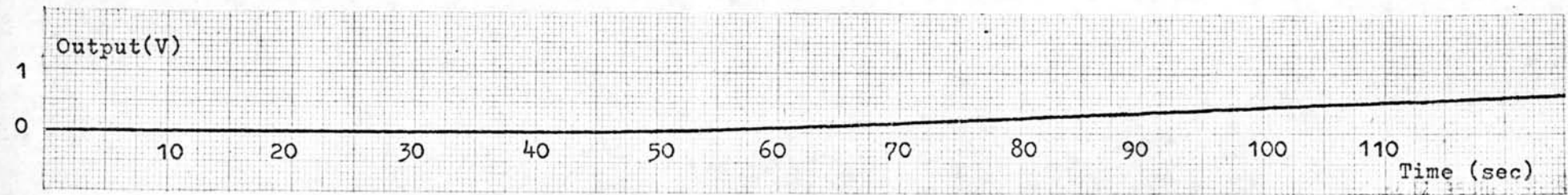
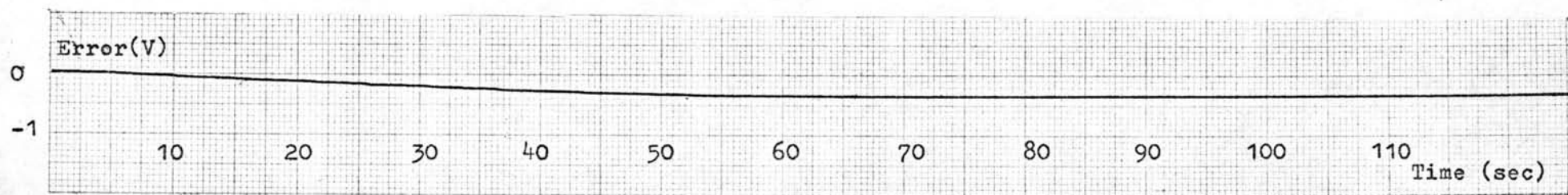
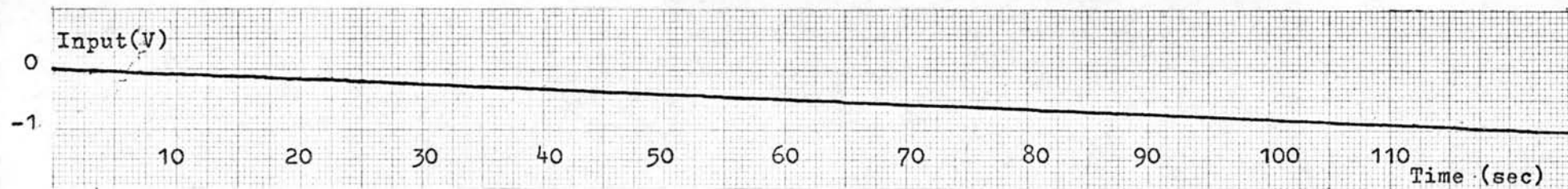
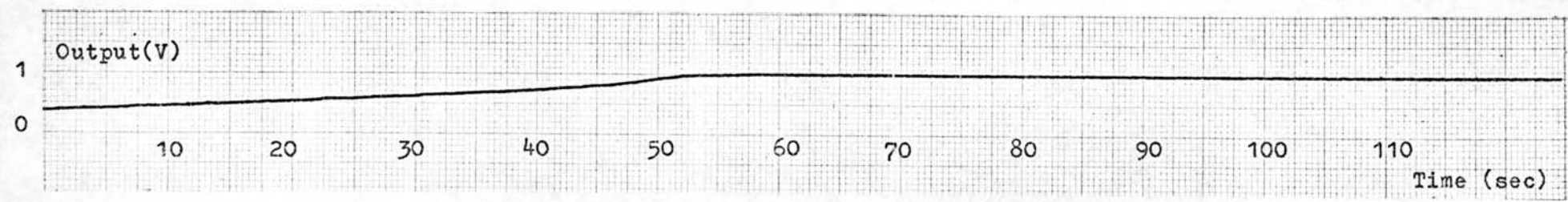
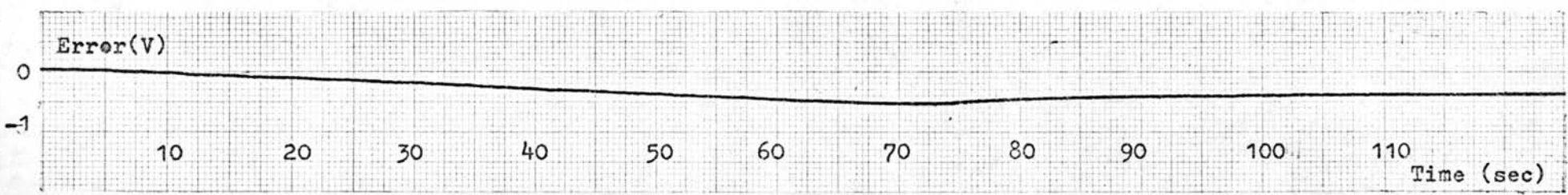
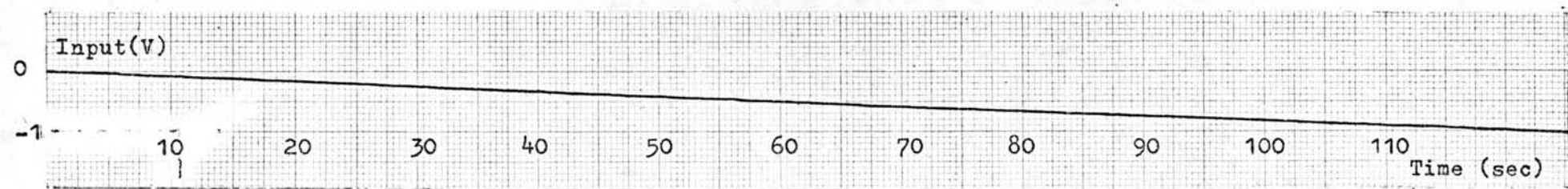
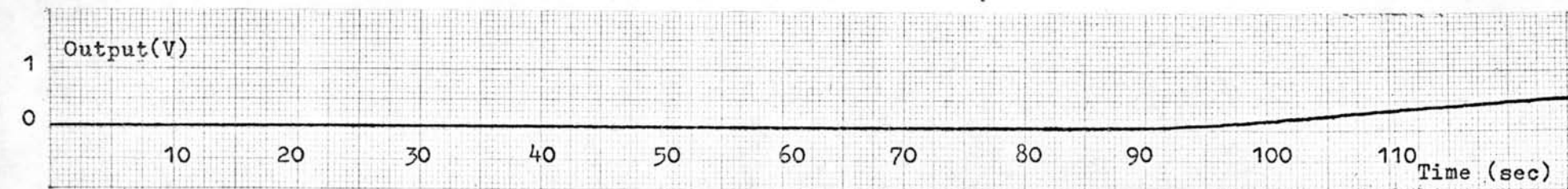
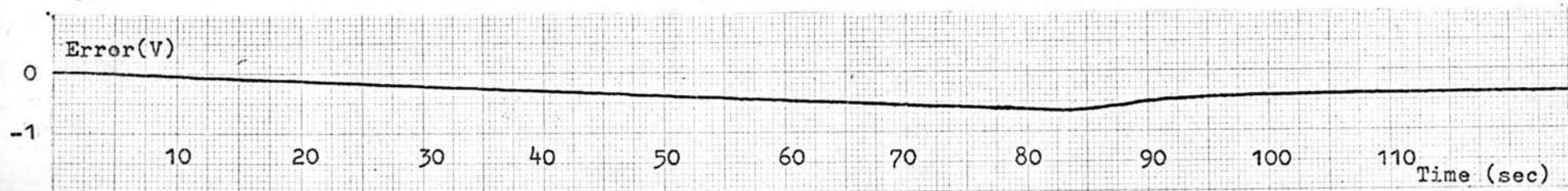
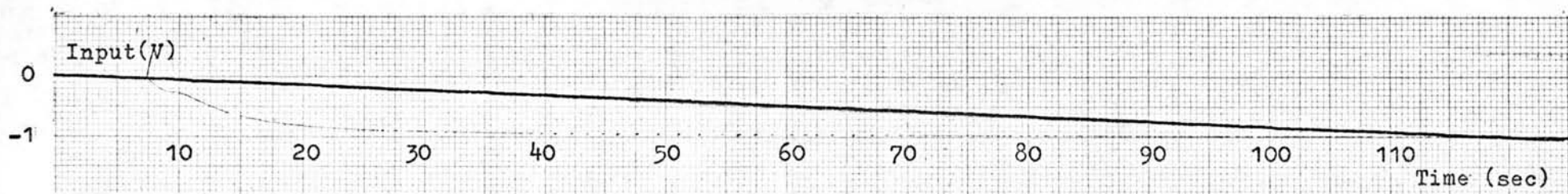


Figure 5.12 (a). Ramp response without backlash



(b). Ramp response with small backlash



(c). Ramp response with larger backlash